

**Population dynamics, relative abundance, and habitat suitability of adult red drum (*Sciaenops ocellatus*) indicate vulnerability to harvest in nearshore waters of the north central Gulf of Mexico**

Crystal LouAllen Hightower<sup>1,2</sup>, J. Marcus Drymon<sup>3,4</sup>, Amanda E. Jefferson<sup>3,4</sup>, Matthew B. Jargowsky<sup>3,4</sup>, Emily A. Seubert<sup>3</sup>, Simon Dedman<sup>5</sup>, John F. Mareska<sup>6</sup>, Sean P. Powers<sup>1,2,\*</sup>

1. University of South Alabama  
Department of Marine Sciences  
5871 USA Drive North  
Mobile, AL 36688, United States

2. Dauphin Island Sea Lab  
101 Bienville Boulevard  
Dauphin Island, AL 36528, United States

3. Mississippi State University  
Coastal Research and Extension Center  
1815 Popp's Ferry Road,  
Biloxi, MS 39532, United States

4. Mississippi-Alabama Sea Grant Consortium  
703 East Beach Drive  
Ocean Springs, MS 39564, United States

5. Stanford University  
Hopkins Marine Station  
120 Oceanview Blvd  
Pacific Grove, CA 93950, United States

6. Alabama Department of Conservation and Natural Resources  
Marine Resources Division  
PO Box 189  
Dauphin Island, AL 36528, United States

\* Corresponding author  
spowers@disl.edu

1 **Abstract**

2 Gulf of Mexico red drum (*Sciaenops ocellatus*) is an immensely popular sportfish, yet is  
3 currently managed as a data-limited stock in federal waters. Despite advances in data-limited  
4 assessments, the most recent federal stock assessment for Gulf of Mexico red drum was not  
5 recommended for providing management advice. Consequently, we sought to address data gaps  
6 highlighted in the assessment by i) producing up-to-date overall and sex-specific growth models,  
7 ii) updating estimates of natural mortality, iii) generating standardized indices of relative  
8 abundance, and iv) providing predictions of habitat suitability. Using a data series from 2006 –  
9 2018, ages ranging from 0 – 36 years were assigned to 1,178 red drum. A negative binomial  
10 generalized linear model including the variables year, depth, surface temperature, dissolved  
11 oxygen, and bottom salinity was used to standardize an index of relative abundance.  
12 Examination of catch per unit effort revealed that adult red drum were significantly more  
13 abundant in state waters relative to federal waters. These findings were well explained by habitat  
14 suitability models, which identified surface velocity, surface temperature, and depth as the  
15 strongest predictors of relative abundance. Collectively, our investigation reveals that the adult  
16 spawning stock is not fully protected by the harvest moratorium in federal waters.

17

18 **Introduction**

19 Advances in data collection approaches and stock assessment techniques have ushered in  
20 the next generation of United States stock assessments (Lynch et al. 2018). For data-rich stocks,  
21 traditional catch and catch per unit effort (CPUE) are increasingly augmented with robust  
22 fishery-independent data sources and ecosystem-based inputs (Lynch et al. 2018), often using  
23 spatially-explicit approaches (e.g., Goethel et al. 2011, Berger et al. 2017). Despite these  
24 advances, more than half of US stocks remain data-limited (Newman et al. 2015). Improving  
25 basic data inputs for data-limited stocks is imperative for increasing the quality of assessments  
26 for these species. For stocks under aggressive rebuilding schedules, where catch data may not  
27 reflect population trends or where harvest is completely restricted, the need for reliable time  
28 series that track abundance is even more critical.

29 Gulf of Mexico (GoM) red drum (*Sciaenops ocellatus*) are a highly prized species  
30 supporting valuable recreational fisheries. Recreational harvest of red drum is permitted in all  
31 GoM state waters (out to 3 nautical miles (nmi) in Louisiana, Mississippi, and Alabama and out  
32 to 9 nmi in Texas and Florida), but a harvest moratorium in federal waters has been in place  
33 since 1987. In addition, commercial harvest is prohibited in all GoM states except Mississippi.  
34 Consequently, the data sources that would be useful for assessing GoM red drum (e.g.,  
35 commercial landings) are lacking (Powers et al. 2012). Thus, despite a wealth of knowledge on  
36 population connectivity (e.g., Rooker et al. 2010), movement and recruitment (e.g., Burnsed et  
37 al. 2020), and spawning (e.g., Lowerre-Barbieri et al. 2019), GoM red drum are classified by  
38 NOAA Fisheries as a “data-limited species” (SEDAR 2016).

39 The 2006 amendment to the Magnuson-Stevens Fishery Conservation and Management  
40 Act required annual catch limits for all federally managed stocks, a mandate that spurred

41 significant advances in the development of data-limited assessment methods (Newman et al.  
42 2015). One of these data-limited methods (DLMtool, Carruthers and Hordyk 2018) was recently  
43 used to assess a suite of data-limited species in the GoM, including lane snapper (*Lutjanus*  
44 *synagris*), wenchman (*Pristipomoides aquilonaris*), yellowmouth grouper (*Mycteroperca*  
45 *interstitialis*), speckled hind (*Epinephalus drummondhayi*), snowy grouper (*E. niveatus*), almaco  
46 jack (*Seriola rivoliana*), lesser amberjack (*S. fasciata*), and red drum (SEDAR 2016). During this  
47 assessment, at least one data-limited method was identified as having preferable performance  
48 compared to the status quo for every species examined, with the notable exception of red drum  
49 (SEDAR 2016). Thus, despite new tools tailored to the assessment of data-limited species,  
50 coupled with a wealth of information about red drum population biology and ecology, the  
51 outputs from this assessment were not recommended for providing management advice for red  
52 drum (SEDAR 2016).

53 While many stocks will inevitably remain data-limited (Newman et al. 2015), careful  
54 examination of existing data deficiencies can improve our ability to assess stocks like GoM red  
55 drum. Specific data recommendations from the most recent red drum assessment included i)  
56 expand efforts to collect age and length samples at varying sizes, seasons, months, and locations,  
57 particularly for offshore fish, ii) identify or optimize fishery-independent surveys to characterize  
58 relative abundance in federal waters, and iii) explore ways to increase data collection from  
59 existing fishery-independent surveys (SEDAR 2016). To that end, the goals of this study were to  
60 combine data from fishery-independent surveys operating throughout the year and across the  
61 continental shelf to i) produce up-to-date overall and sex-specific growth models, ii) update  
62 estimates of natural mortality, iii) generate standardized indices of relative abundance, and iv)

63 provide predictions of habitat suitability for red drum in the north central GoM, which can then  
64 be used to optimize future fishery-independent surveys.

65

## 66 **Materials and Methods**

### 67 *Data collection*

68 Catch data for adult red drum were collected as part of fishery-independent bottom  
69 longline surveys conducted during spring, summer, autumn, and winter in the north central GoM  
70 from 2006 – 2018 (Figure 1). Bottom longline locations were selected using a stratified-random  
71 sampling design and sampled following standardized methods described in Drymon et al. (2013,  
72 2020). Briefly, the main line consisted of 1.85 km (1 nmi) of 4 mm monofilament (545 kg test)  
73 that was set with 100 gangions. Gangions consisted of a longline snap and a 15/0 circle hook  
74 baited with Atlantic mackerel (*Scomber scombrus*). Each gangion was made of 3.66 m of 3 mm  
75 monofilament (320 kg test). All sets were soaked for 1 hour and mid-set measurements of  
76 surface and bottom temperature (°C), salinity (psu), and bottom dissolved oxygen (mg l<sup>-1</sup>), as  
77 well as start and end set-depth (m), were recorded. During the bottom longline retrieval, all red  
78 drum encountered were measured to the nearest mm (maximum total length), weighed, and  
79 retained red drum were sexed. Sagittal otoliths were extracted for age and growth analyses.

80 Catch data were converted to CPUE, expressed as the number of individuals 100 hooks<sup>-1</sup> hour<sup>-1</sup>.

81 To augment the collection of adult red drum from the bottom longline survey, smaller red  
82 drum were collected and aged from the Alabama Department of Conservation and Natural  
83 Resources, Marine Resources Division (AMRD) monthly gillnet survey from 2006 – 2018. This  
84 survey included areas of Coastal Alabama from eastern Mississippi Sound to western Perdido  
85 Bay and Mobile Bay (Figure 1; Livernois et al. 2020). The AMRD gillnet survey involves two

86 different nets: a small mesh gillnet and a large mesh gillnet. The small mesh gillnet consists of 5  
87 panels that are 45.0 m long by 2.4 m deep, each containing stretch meshes ranging in size from  
88 5.1 – 10.2 cm. The large mesh gillnet consists of 4 panels that are also 45.0 m long by 2.4 m  
89 deep, with stretch meshes ranging in size from 11.4 – 15.2 cm. Red drum caught in either gillnet  
90 were measured to the nearest mm (maximum total length), weighed, and sexed. Sagittal otoliths  
91 were extracted for age and growth analyses.

92 For all ages combined (longline and gillnet), two-sample Kolmogorov-Smirnov tests  
93 were used to examine differences in length and weight distributions between sexes. Some  
94 longline-collected red drum lacked total length measurements. For longline-collected red drum  
95 that had both maximum total and fork length measurements, maximum total length was  
96 regressed on fork length, resulting in the equation:

$$97 \quad \text{Total Length} = 1.04(\text{Fork Length}) + 23.53 \quad (1)$$

98 where total and fork lengths are expressed in millimeters ( $n = 346$ ,  $R^2 = 0.96$ ). This regression  
99 was used to estimate lengths of longline-collected red drum that were lacking a maximum total  
100 length measurement ( $n = 238$ ).

#### 101 *Otolith processing and aging*

102 All otoliths were processed following procedures detailed in Powers et al. (2012) and  
103 VanderKooy et al. (2020). A portion of the fish aged in Powers et al. (2012) were also included  
104 in the present study; however, these fish were re-aged during the present study for consistency.  
105 Once otoliths were processed, aging was conducted independently (without consulting the other  
106 reader) and blindly (without knowledge of fish capture date or size) by two readers. Each otolith  
107 section was viewed using a stereomicroscope with transmitted light (brightfield illumination).  
108

109 The number of opaque zones was counted along the ventral edge of the sulcus acusticus. A  
110 margin code (1 – 4) was assigned to the otolith margin according to the Gulf of Mexico Marine  
111 Fisheries Commission (GSMFC) otolith manual (VanderKooy et al. 2020).

112 Whole age, in years, was calculated for each fish according to GSMFC guidelines. If the  
113 collection month was January – June and the margin code was 3 or 4, then the whole age equaled  
114 the number of opaque zones, plus 1. If the collection month was October – December and the  
115 margin code was 1 or 2, then the whole age equaled the number of opaque zones, minus 1. For  
116 all other combinations of capture month and margin code, the whole age equaled the number of  
117 opaque zones. Next, the number of days between the capture date and October 1 (the assumed  
118 birthdate of red drum; Ditty 1986) of the previous year were calculated. This number was then  
119 divided by the total number of days in the capture year, and the result was added to the whole  
120 age to yield the fractional age.

121 If any otolith was assigned different whole ages, the readers consulted with each other or  
122 a third reader aged the otolith. If the two initial readers did not reach an agreement, or if the third  
123 reader did not agree with one of the two initial readers, the otolith was excluded from further  
124 analysis. Average percent error (APE) was calculated for all whole ages to evaluate between-  
125 reader precision (Beamish and Fournier 1981, Campana 2001). Two-sample Kolmogorov-  
126 Smirnov tests were used to examine differences in fractional age distributions between sexes.

127

### 128 *Modeling growth*

129 To estimate growth parameters for red drum in this study, the von Bertalanffy growth  
130 function (VBGF) was fit to female, male, and unknown sexed red drum for the complete data set,

131 fishery-independent AMRD gillnet data set, and bottom longline data set using the following  
132 equation:

$$133 \quad L_t = L_\infty(1 - e^{-K(t-t_0)}) \quad (2)$$

134 where  $L_t$  = predicted total length in millimeters,  $L_\infty$  = mean asymptotic length in millimeters,  $K$  =  
135 Brody growth rate coefficient in years<sup>-1</sup>,  $t$  = time (fractional age) in years, and  $t_0$  = hypothetical  
136 age at which length equals 0 in years (von Bertalanffy 1938).

137 The VBGF was used to model sex-specific growth. Eight candidate versions of the  
138 VBGF were fit to the sex-specific fractional age data: a general version, where all three  
139 parameters ( $L_\infty$ ,  $K$ , and  $t_0$ ) could vary between sexes; three versions where two of the three  
140 parameters could vary between sexes; three versions where only one parameter could vary  
141 between sexes; and a common version where all three parameters were held constant between  
142 sexes (Ogle 2016, Nelson et al. 2018, Jefferson et al. 2019). Akaike's Information Criterion  
143 (AIC) was used to rank these models based on fit and to identify the best-fitting version (Akaike  
144 1998, Katsanevakis and Maravelias 2008, Ogle 2016). All growth parameters were modeled in  
145 the R v3.6.3 language and software environment (R Core Team 2020) using the add-on packages  
146 *FSA* (Ogle et al. 2020) and *nlstools* (Baty et al. 2015).

#### 147 148 *Estimating mortality*

149 Using whole ages of bottom longline specimens, an age-based catch curve (Chapman and  
150 Robson 1960) was created for calculating total mortality; however, graphical examination of the  
151 catch curve revealed that critical assumptions necessary for estimating instantaneous total  
152 mortality had been violated (Tuckey et al. 2007, Smith et al. 2012). Specifically, red drum did  
153 not appear to fully recruit to the gear until age 20, so any mortality estimates generated from this

154 catch curve would not be representative of the stock. Although total mortality estimates were  
155 unattainable, instantaneous natural mortality rate ( $M$ ) was calculated using three empirical  
156 methods (Then et al. 2015, Ogle 2016):

157 1. Hoenig<sub>fishes</sub>, Hoenig's (1983) log-transformed linear regression for fishes:

158 
$$M = e^{1.46 - 1.01 \log_e(t_{max})}, \quad (3)$$

159 where  $t_{max}$  is the maximum age of the animal in years;

160 2. The Hoenig<sub>nls</sub> (non-linear least squares) estimator (Then et al. 2015):

161 
$$M = 4.899 t_{max}^{-0.916}, \quad (4)$$

162 where  $t_{max}$  is the maximum age of the animal in years; and

163 3. The Pauly<sub>nls-T</sub> (non-linear least squares, omitting temperature) estimator (Pauly 1980,

164 Then et al. 2015):

165 
$$M = 4.118 K^{0.73} L_{\infty}^{-0.333}, \quad (5)$$

166 where  $K$  and  $L_{\infty}$  are parameters from the combined VBGF. All mortality analyses were  
167 conducted in R using *FSA*.

168

### 169 *Relative abundance*

170 Yearly changes in CPUE for red drum sampled during the bottom longline survey were  
171 examined by generating a nominal index of relative abundance. To standardize the index of  
172 relative abundance, a negative binomial generalized linear model (nbGLM) (Hardin and Hilbe  
173 2007) was fit to the CPUE data using the *glmmTMB* package (Brooks et al. 2017) in R. Abiotic  
174 variables thought to influence CPUE were added to the model using forward step-wise model  
175 selection. Akaike's Information Criterion was used to identify the best-fitting model. Model fit  
176 was examined by using the *DHARMA* package (Hartig 2017) in R to check for uniformity,

177 outliers, dispersion, and zero-inflation. Multicollinearity was tested using the *performance*  
178 package (Lüdecke et al. 2019) in R, with variance inflation factors (VIFs) less than 10 signifying  
179 low correlation (Dormann et al. 2013). To create a standardized yearly index, the abiotic  
180 variables thought to influence CPUE were set to their median values.

181

### 182 *Spatial analysis*

183 The index of relative abundance generated above was used to examine trends in red drum  
184 relative abundance. First, minimum distance from shore (km) was calculated in QGIS (Quantum  
185 GIS Development Team 2019). Then, nominal CPUE was calculated for four discrete areas: less  
186 than 3 nmi from shore (i.e., state waters), 3 – 6 nmi from shore, 6 – 9 nmi from shore, and  
187 greater than 9 nmi from shore. Finally, a one-way ANOVA, followed by a Tukey multiple  
188 pairwise-comparisons test, was used to test for differences in nominal CPUE between these four  
189 areas. Age and length versus distance from shore were also examined to identify the composition  
190 of red drum vulnerable to recreational fishermen in state waters versus those protected in federal  
191 waters.

192

### 193 *Habitat modeling*

194 Boosted regression trees (BRTs) were used to describe the relationships between the  
195 CPUE of red drum from the bottom longline survey and environmental variables potentially  
196 influencing distribution and abundance. Specifically, BRTs were fit for three seasons  
197 (meteorological spring, summer, and autumn); winter data were not included in BRT analyses  
198 given few red drum captured ( $n = 35$ ) and relatively low effort ( $n = 70$  stations). Boosted  
199 regression trees use machine learning to fit complex, non-linear relationships and offer predictive

200 advantages over generalized linear or additive models (GLMs and GAMs). For a complete  
201 description of BRTs and the methods used in this study, see Drymon et al. (2020).

202 Preliminary analyses indicated a high proportion of zero values (i.e., zero-inflated data).  
203 To account for the preponderance of zeros, a two-step (i.e., delta or hurdle) process was chosen  
204 to model catch data. Presence/absence probability was modeled using a BRT with a binary  
205 distribution and continuous non-zero (i.e., abundance) probability was modeled using a BRT  
206 with a Gaussian distribution. Because the catch data also contained some instances of  
207 anomalously high catch (i.e., long-tailed data), non-zero data were natural log-transformed.  
208 Predictions were reverse log-transformed so that the final model is a product of the binary and  
209 Gaussian BRTs (Lo et al. 1992).

210 Sixteen variables from multiple sources were considered for the BRT models  
211 (Supplemental Table 1). While some variables (e.g., temperature, salinity and dissolved oxygen)  
212 were collected on-site during bottom longline sampling, all predictor data were obtained  
213 following methods outlined in Drymon et al. (2020) to facilitate comparisons with previous  
214 habitat modeling in the same region. Surface and bottom temperature (°C), salinity (psu), and  
215 three-dimensional surface and bottom current velocity (surface, northward, upward; m/s), as well  
216 as sea surface height (m), were obtained from the Hybrid Coordinate Ocean Model (HYCOM)  
217 data server (4 km resolution). Bottom dissolved oxygen ( $\text{mg l}^{-1}$ ) was obtained from the National  
218 Oceanic and Atmospheric Administration (NOAA)<sup>1</sup> and interpolated across ~100 – 250 survey  
219 stations (number varied by year). Depth (m) and substrate grain size (mm) were obtained from  
220 the United States Geological Survey (USGS)<sup>2</sup>, 0.33 arc seconds, (~10 m resolution). Daylength

---

<sup>1</sup> <https://www.ncddc.noaa.gov/hypoxia/products/2010>

<sup>2</sup> [http://pubs.usgs.gov/ds/2006/146/basemaps/gmx\\_grd/gmx\\_grd.zip](http://pubs.usgs.gov/ds/2006/146/basemaps/gmx_grd/gmx_grd.zip)

221 (min) was calculated in R using code by Simon Dedman<sup>3</sup>. Given the quantity of potential  
222 predictor data considered within the BRT models, some degree of spatial autocorrelation was  
223 anticipated (e.g., between distance from shore and depth, between surface and bottom  
224 temperature, etc.); however, BRTs are robust to autocorrelation among independent variables  
225 (Abeare 2009). All BRT models were fit using the package *gbm.auto* (Dedman et al. 2017) in R.  
226 Learning rate (lr), bag fraction (bf), and tree contribution (tc) are parameters that are used in  
227 concert to achieve minimum predictive error (Elith et al. 2008). These were optimized using  
228 *gbm.auto* for each season model run.

229

### 230 *Model performance and interpretation*

231 The BRT modeling approach automatically partitioned the data into training and testing  
232 sets, a ratio dictated by the bag fraction. Ten-fold cross-validation (CV) was then performed,  
233 with the members of the training/testing sets randomized each time. Performance metrics  
234 included training/testing correlation, CV deviance (and standard error (SE)) and correlation (and  
235 SE), as well as Area Under Receiver-Operator-Curve (AUC) and its CV and CV SE for the  
236 binary models (Parisien and Moritz 2009). The final Gaussian fitted functions from the BRT  
237 were visualized using marginal effect plots to indicate the effect of a particular variable on the  
238 response after accounting for the average effects of other model variables (Elith et al. 2008).

239

### 240 *Habitat suitability*

241 The distribution of suitable habitat was predicted via the BRTs described above.  
242 Environmental data for model predictions were obtained as detailed above, except that HYCOM

---

<sup>3</sup> [www.github.com/SimonDedman/daylength](http://www.github.com/SimonDedman/daylength)

243 data were extracted for one representative date per season (monthly groupings per each season,  
244 i.e., MAM/JJA/SON) at a resolution of 4 km. Representative dates for environmental data were  
245 selected by ranking the absolute value of the differences of all sites' values for all variables  
246 against the mean for those variables, then identifying the date within each season that most  
247 closely matched those values. The BRT models then generated predictive CPUE values for each  
248 2 km × 2 km cell. These values were then then mapped in QGIS using the heatmap setting to  
249 produce color points weighted by the predicted abundances generated from the BRT. Using  
250 *gbm.auto*, the coefficient of variance was calculated for the predicted abundance values at each 2  
251 km x 2 km cell to represent model variance.

## 253 **Results**

### 254 *Catch data*

255 Between May 2006 and November 2018, 1,296 bottom longline sets were conducted and  
256 815 red drum were caught (Figure 2), 741 of which were measured and 472 of which were kept  
257 for otolith collection. Approximately 100 stations were sampled each year (mean = 100, SD =  
258 22, range 80-143), and survey effort (number of sets) was relatively well distributed across the  
259 three seasons examined in the BRTs: spring (n = 460), summer (n = 405), and autumn (n = 361).  
260 Red drum caught on the bottom longline were primarily encountered in state waters across all  
261 seasons (Figure 2) and were exclusively larger than size at 50% maturity according to Bennetts  
262 et al. (2019) (Figure 3A).

263 To supplement the 472 red drum retained from the bottom longline, otoliths from an  
264 additional 709 gillnet-captured red drum were analyzed, thus providing a total of 1,181 red drum  
265 for age and growth analyses. Of these fish, 392 were female, 369 were male, and 420 were

266 unknown sex. The female-to-male ratio was 1.06:1 and did not differ significantly from a 1:1  
267 ratio ( $X^2 = 0.70$ ,  $DF = 1$ ,  $P = 0.40$ ). Total length ranged from 80 – 1102 mm (Figure 3B). The  
268 average ( $\pm$  SE) total length of all specimens (bottom longline and gillnet combined) was 619.13  
269  $\pm$  8.22 mm. Kolmogorov-Smirnov tests revealed that females were significantly longer ( $D =$   
270  $0.20$ ,  $P < 0.01$ ) and heavier ( $D = 0.18$ ,  $P < 0.01$ ) than males.

271

## 272 *Age*

273 Ages were assigned to 1,178 red drum. Otoliths from the remaining 3 fish (0.25% of all  
274 specimens) were deemed unreadable and were omitted from further analysis. Four fish had no  
275 length measurements and were also omitted from further analysis. The between-reader percent  
276 agreement was 93.46% and the between-reader APE was 4.52%; these estimates were largely  
277 driven by differences in the margin codes assigned to age-0 fish. Whole age ranged from 0 – 36  
278 years and fractional age ranged from 0.37 – 36.53 years. The maximum age of both sexes was 36  
279 years; however, Kolmogorov-Smirnov tests showed that fractional age distributions differed  
280 significantly by sex ( $D = 0.15$ ,  $P < 0.01$ ). The mean ages of females and males were 11.72 and  
281 9.90 years, respectively.

282

## 283 *Growth and mortality*

284 The VBGF equation for all age data combined (including females, males, and unknown  
285 sex) is

$$286 \quad l_t = 950.45(1 - e^{-0.31(t-(-0.26))}) \quad (\text{Figure 4A}). \quad (6)$$

287 For the sex-specific data, the model version which allowed  $L_\infty$  and  $t_0$  to vary by sex (“fit2L2T”)  
288 best fit the data. “Fit2L2T” was followed closely by “fit2L2K” ( $L_\infty$  and  $K$  vary;  $\Delta AIC = 1.7$ ) and

289 “fitGeneral” (all parameters vary;  $\Delta AIC = 1.7$ ). Based on “fit2L2T,” females have a higher  $L_{\infty}$   
290 value compared to males. The VBGF equations for female and male red drum, respectively, are

291 
$$l_{t(F)} = 969.63(1 - e^{-0.30(t-(-0.35))}) \quad (7)$$

292 and

293 
$$l_{t(M)} = 932.71(1 - e^{-0.30(t-(-0.45))}) \text{ (Figure 4B).} \quad (8)$$

294 All VBGF parameters from the present study are listed in Table 1. Estimates of  $M$  were as  
295 follows:  $\text{Hoenig}_{\text{fishes}} = 0.12$ ,  $\text{Hoenig}_{\text{nls}} = 0.14$ , and  $\text{Pauly}_{\text{nls-T}} = 0.39$ .

296

297 *Relative abundance*

298 The final version of the nbGLM included the variables year, depth, surface temperature,  
299 dissolved oxygen, and bottom salinity. The variables latitude, longitude, bottom temperature,  
300 surface salinity, and daylength were also tested but were excluded from the final version of the  
301 model. Model fit was deemed appropriate as the model did not suffer from deviations from  
302 uniformity, outliers (Supplemental Figure 1), dispersion ( $P = 0.92$ ), or zero-inflation ( $P = 0.87$ ).

303 The VIF analysis indicated a lack of multicollinearity, as all VIFs were less than 2. Year was not  
304 significant ( $P = 0.13$ ) and there were no trends within the standardized index (Figure 5),

305 indicating that the declines in the nominal CPUE data from 2007 – 2010 reflect increases in  
306 offshore sampling effort beginning in 2010 rather than changes in red drum relative abundance.

307

308 *Spatial analysis*

309 From 2006 – 2018, bottom longline sets were distributed fairly evenly between state  
310 (46%) and federal (54%) waters. Nominal CPUE ( $\pm$  SE, number of stations) was highest less

311 than 3 nmi from shore ( $1.13 \pm 0.10$ ,  $n = 602$ ), followed by 3 – 6 nmi from shore ( $0.72 \pm 0.18$ ,  $n =$   
312 103), 6 – 9 nmi from shore ( $0.35 \pm 0.19$ ,  $n = 58$ ), and greater than 9 nmi from shore ( $0.08 \pm 0.03$ ,  
313  $n = 533$ ). The one-way ANOVA found that distance from shore was significant ( $P < 0.01$ ). The  
314 Tukey multiple pairwise-comparisons test indicated that nominal CPUE was significantly higher  
315 less than 3 nmi from shore compared to 6 – 9 nmi from shore ( $P < 0.01$ ) and greater than 9 nmi  
316 from shore ( $P < 0.01$ ). Nominal CPUE was also significantly higher 3 – 6 nmi from shore  
317 compared to greater than 9 nmi from shore ( $P < 0.01$ ). Both age ( $D = 0.414$ ,  $P < 0.01$ ) and length  
318 distributions ( $D = 0.422$ ,  $P < 0.01$ ) were significantly different for red drum caught in state  
319 versus federal waters. Notably, fish were older and larger in state waters (average age of 18 years  
320 and average length of 938 mm) compared to federal waters (average age of 12 years and average  
321 length of 887 mm). Further examination revealed a negative correlation between age and  
322 distance from shore ( $r = -0.239$ ,  $P < 0.01$ ) and size and distance from shore ( $r = -0.274$ ,  $P <$   
323 0.01).

#### 325 *Model performance and interpretation*

326 Model performance was assessed for all red drum across the three sampling seasons:  
327 spring, summer, and autumn. Training data AUC scores were high across all seasons (0.90),  
328 indicating very good model performance according to criteria defined in Lane et al. (2009)  
329 (Table 2). Cross-validated AUC scores ( $\pm$  SE) were 0.85 – 0.86 ( $\pm 0.01$ ), indicating that model  
330 overfitting was negligible (Hijmans and Elith 2013).

331

#### 332 *Habitat suitability*

333 Across all seasons, surface northward velocity, surface temperature, and depth were the  
334 three most influential predictors of red drum abundance (Table 2). In particular, red drum  
335 showed a preference for surface northward velocities greater than 0 m/s, with high preferences  
336 for velocities greater than 0.1 m/s (Figure 6A, D, G). Preferences for surface temperatures less  
337 than 22°C (Figure 6B, E, H) and depths between 5 and 17 m (Figure 6C, F, I) were also  
338 apparent. These predictors were consistent across seasons. In general, the most suitable habitat  
339 for red drum was predominately within state waters. A seasonal shift in predicted habitat  
340 suitability was detected, suggesting red drum prefer shallower habitats in the spring and autumn  
341 as opposed to deeper waters during the summer (Figure 7). Coefficients of variance of the  
342 predicted relative abundance were low, but were highest in deeper waters (Supplemental Figure  
343 2). Since all fish in the BRT analysis were larger than size at 50% maturity (Figure 3A), we are  
344 confident that these results do not confound localized spatial preferences with life-history shifts  
345 in habitat use.

346

## 347 **Discussion**

348 Our findings, based on a large sample size and broad size distribution, support previous  
349 studies indicating that GoM red drum are a relatively long-lived, slow-growing species. Perhaps  
350 not surprisingly, our findings are most similar to those of Bennetts et al. (2019); both studies  
351 used three-parameter VBGFs to model sex-specific growth from a similar number and size range  
352 of fish in Mississippi and Alabama. However, the maximum age reported in the present study is  
353 notably older than the maximum age reported by Bennetts et al. (2019) (36 vs. 31 years), a  
354 difference that illustrates the importance of sampling enough large, presumably old individuals.  
355 Specifically, we collected more than 4 times more individuals larger than 1000 mm TL than

356 Bennetts et al. (2019); two of these fish, one male and one female, were assigned ages of 36  
357 years. While fish older than 36 are likely rare off Mississippi and Alabama, future efforts to  
358 model age and growth for red drum should consider collections that span the entirety of the  
359 species' range, as well as account for the effects of gear selectivity, temporal or spatial changes  
360 in age structure, variable recruitment, and unexplained variance arising from unsexed  
361 individuals, all of which are potential sources of growth model parameter bias in the current  
362 study.

363         Despite the large sample size and broad size distribution captured using two fishery-  
364 independent gear types, individuals between 600 and 800 mm TL (ages 3 – 6) were notably rare  
365 in our study. Interestingly, this is precisely when red drum in this region undergo maturation,  
366 according to mean size- and age-at-maturity estimates from Bennetts et al. (2019). Specifically,  
367 mean age at 50% maturity for males and females is approximately 3 years, with fully mature  
368 individuals (spawning capable and elevated GSI) undetected until ages 5 and 6 (Bennetts et al.  
369 2019). Thus, while a multi-panel gillnet adequately samples ages 0 – 2, and the bottom longline  
370 adequately samples fish aged 7 and older, fish between the ages of 3 and 6 aren't selected for by  
371 either gear type. Similar size selectivity been shown for red drum off the west Florida shelf.  
372 Using three fishery-independent gear types (haul seine, trammel net, and purse seine), Winner et  
373 al. (2014) demonstrated that 600 – 800 mm red drum were not well represented in either haul  
374 seines or purse seines, yet were dominant in trammel net surveys. These examples illustrate the  
375 difficulty in assessing red drum and suggest that multiple gear types are needed to describe  
376 population dynamics across all life stages of this species.

377         Surprisingly, a comprehensive review of red drum life history studies revealed that recent  
378 age-based natural mortality estimates are lacking for this species (SEDAR 2016). During the

379 assessment, it was concluded that the updated Hoenig equation using longevity (Then et al.  
380 2015) was the most robust approach for red drum. Our estimate of instantaneous annual natural  
381 mortality based on the Then et al. (2015) approach was  $0.14 \text{ y}^{-1}$ , which is similar to the range of  
382 values used in the assessment ( $0.16 \text{ y}^{-1} - 0.18 \text{ y}^{-1}$ ). Unfortunately, the current assessment  
383 approach (DLMtool, Carruthers and Hordyk 2018) does not allow for age-dependent estimates of  
384 M. This is potentially problematic for red drum, as fishing pressure is higher for juveniles, which  
385 likely experience different natural mortality rates relative to older individuals. As red drum  
386 become less data-limited, developing the ability to account for age-based differences in natural  
387 mortality should be prioritized.

388         The development of a gulf-wide index of relative abundance generated from fishery-  
389 independent bottom longline surveys is critical for future assessments of red drum. During the  
390 last assessment, six potential methods were considered for generating catch advice. The only  
391 method to meet the performance criteria was Islope, which is solely based on an index of relative  
392 abundance (Carruthers and Hordyk 2018). For GoM red drum, the index of relative abundance  
393 deemed most representative of the adult spawning stock was the index based upon our bottom  
394 longline survey. Thus, the index of relative abundance generated in this study is an important  
395 step toward producing catch advice for this data-limited species. This index suggests that the  
396 relative abundance of red drum has varied little over the past thirteen years. However, given the  
397 long lifespan of red drum, changes in relative abundance for this species are likely to be delayed  
398 and gradual. Consequently, continued fishery-independent monitoring is essential, both for  
399 characterizing changes in the population and for increasing the stability of catch advice  
400 generated from future assessments that apply the Islope approach (Sagarese et al. 2018).

401 Current management of red drum in the GoM relies on each GoM state meeting an  
402 escapement goal (30%) of 4-year-old red drum. The premise of this management scheme is that  
403 most of these fish would enter the offshore adult population where the federal moratorium on  
404 GoM red drum protects the adult spawning stock. However, CPUE for adult red drum was  
405 substantially higher in state waters than in federal waters. This has been shown in other areas of  
406 the GoM (e.g., Winner et al. 2014) and along the east coast of Florida (Reyier et al. 2011),  
407 particularly from August to November when adults return to state waters to spawn (Lowerre-  
408 Barbieri et al. 2016 and 2018). These individuals travel to localized natal areas where they are  
409 targeted within spawning aggregations (Burnsed et al. 2020). Although state-level management  
410 for red drum is primarily focused on regulating the harvest of juveniles using slot limits, the  
411 current management plans for four out of five GoM states (i.e., except Florida) also afford  
412 opportunities to keep a red drum larger than the slot limit. For example, landings data from the  
413 Marine Recreational Information Program (MRIP 2021) demonstrate that nearly 20% of redfish  
414 taken from Mississippi and Alabama state waters are greater than 30 inches fork length, whereas  
415 no fish this size are landed in Florida (Figure 8). Our findings clearly demonstrate that off the  
416 coast of Alabama, the federal moratorium does not protect the larger, older age classes of red  
417 drum from harvest. Adequately protecting these fish will require state management measures that  
418 either completely prohibit the harvest of large individuals (e.g., Florida) or impose a tag system  
419 that allows a single over-slot fish per year (e.g., Texas).

420 The catch data support the outputs from the BRTs, which indicate that adult red drum  
421 prefer inshore, state waters. It is long established that red drum spawning schools aggregate near  
422 tidal passes (Lowerre-Barbieri et al. 2008, Reyier et al. 2011); our analysis provides a  
423 mechanistic explanation for this observation, confirming the importance of surface current

424 velocity when defining suitable habitat for red drum. Temperature is also well known as a strong  
425 predictor of red drum habitat use. Previous work from this region documented bimodal peaks in  
426 relative abundance in the spring and autumn and noted that these peaks corresponded to  
427 temperatures of 21 and 20 degrees, respectively (Powers et al. 2012), which are consistent with  
428 the preferred temperature values identified in this study. Based on the habitat suitability  
429 predictions from the BRTs, we speculate that during the summer, adult red drum may be using  
430 deeper, cooler waters as a thermal refuge.

### 431 **Conclusions**

432 Clearly, assessing a stock under a complete harvest moratorium presents distinct  
433 challenges. Nonetheless, when the data typically used to assess stock status (e.g., commercial  
434 catch data) are lacking, an opportunity exists to consider alternative data sources, which can  
435 sometimes provide new information about stock dynamics (Olney and Hoenig 2001). Such is the  
436 case for GoM red drum. In addition to updated ages, growth models, and natural mortality  
437 estimates, our investigation reveals that the adult spawning stock is not fully protected by the  
438 federal harvest moratorium. Moreover, our habitat suitability models identify factors that may  
439 predict suitable habitat for red drum in other regions of the GoM. Collectively, the findings from  
440 this study, in concert with future efforts to combine nearshore indices of relative abundance from  
441 standardized bottom longline surveys throughout the region (e.g., SEAMAP), will be critical for  
442 advancing GoM red drum from its status as a data-limited stock.

443

### 444 **Acknowledgments**

445 We thank Dauphin Island Sea Lab captains and crew, especially Captains T Guoba and J  
446 Wittmann, for their help with the bottom longline survey. We thank A Kroetz, T Spearman, TR  
447 Nelson and others for their help with field collections, otolith processing, and aging. Thanks to

448 the Alabama Marine Resources Division for collecting and sharing red drum gillnet data. This  
449 work was conducted in accordance with IACUC protocol #1562086 and was funded in part by  
450 the Gulf of Mexico Fishery Management Council.

Draft in Review

451 **Literature Cited**

- 452 Abeare, S.  
453 2009. Comparisons of Boosted Regression Tree, GLM and GAM Performance in the  
454 Standardization of Yellowfin Tuna Catch-Rate Data from the Gulf of Mexico Online  
455 (sic) Fishery. Master's thesis, Louisiana State University, Baton Rouge, LA.  
456
- 457 Akaike, H.  
458 1998. Information theory and an extension of the maximum likelihood principle. Pages 199–  
459 213 in E. Parzen, K. Tanabe, and G. Kitagawa, editors. Selected papers of Hirotugu  
460 Akaike. Springer, New York.  
461
- 462 Baty, F., C. Ritz, S. Charles, M. Brutsche, J.-P. Flandrois, and M.-L. Delignette-Muller.  
463 2015. A toolbox for nonlinear regression in R: the package nlstools. *Journal of Statistical*  
464 *Software* 66:1–21.  
465
- 466 Beamish, R. J., and D. A. Fournier.  
467 1981. A method for comparing the precision of a set of age determinations. *Can. J. Fish.*  
468 *Aquat. Sci.* 38:982–983.  
469
- 470 Bennetts, C. F., R. L. Leaf, and N. J. Brown-Peterson.  
471 2019. Sex-specific growth and reproductive dynamics of Red Drum in the northern Gulf of  
472 Mexico. *Mar. Coast. Fish.* 11:213–230.  
473
- 474 Berger, A. M., Goethel, D. R. and Lynch, P. D.  
475 2017. Introduction to “space oddity: recent advances incorporating spatial processes in the  
476 fishery stock assessment and management interface”. *Can. J. Fish. Aquat. Sci.*  
477 74(11), pp.1693-1697.  
478
- 479 Brooks, M. E., K. Kristensen, K. J. van Benthem, A. Magnusson, C.W. Berg, A. Nielsen, H. J.  
480 Skaug, M. Machler, and B. M. Bolker.  
481 2017. glmmTMB balances speed and flexibility among packages for zero-inflated  
482 generalized linear mixed modeling. *The R Journal* 9(2):378–400.  
483
- 484 Burnsed, S. W., Lowerre-Barbieri, S., Bickford, J. and Leone, E. H.  
485 2020. Recruitment and movement ecology of red drum *Sciaenops ocellatus* differs by natal  
486 estuary. *Mar. Ecol. Prog. Ser.* 633, pp.181-196.  
487
- 488 Campana, S. E.  
489 2001. Accuracy, precision and quality control in age determination, including a review of  
490 the use and abuse of age validation methods. *J. Fish. Biol.* 59:197–242.  
491
- 492 Carruthers, T. R. and Hordyk, A. R.  
493 2018. The Data-Limited Methods Toolkit (DLM tool): An R package for informing  
494 management of data-limited populations. *Methods Ecol. Evol.* 9(12), pp.2388-2395.  
495

496 Chapman, D. G., and D. S. Robson.  
 497 1960. The analysis of a catch curve. *Biometrics* 16:354–368.  
 498

499 Dedman, S., R. Officer, M. Clarke, D. G. Reid, and D. Brophy.  
 500 2017. Gbm.auto: a software tool to simplify spatial modelling and Marine Protected Area  
 501 planning. *PLoS One* 12:e0188955. doi: 10.1371/journal.pone.0188955  
 502

503 Ditty, J. G.  
 504 1986. Ichthyoplankton in neritic waters of the northern Gulf of Mexico off Louisiana:  
 505 composition, relative abundance, and seasonality. *Fish. Bull.* 84:935–946.  
 506

507 Dormann, C. F., J. Elith, S. Bacher, C. Buchmann, G. Carl, G. Carré, et al.  
 508 2013. Collinearity: a review of methods to deal with it and a simulation study evaluating  
 509 their performance. *Ecography* 36:27–46. doi: 10.1111/j.1600-0587.2012.07348.x  
 510

511 Drymon, J. M., L. Carassou, S. P. Powers, M. Grace, J. Dindo, and B. Dzwonkowski.  
 512 2013. Multiscale analysis of factors that affect the distribution of sharks throughout the  
 513 northern Gulf of Mexico. *Fish. Bull.* 111:370–380. doi: 10.7755/fb.111.4.6  
 514

515 Drymon, J. M., S. Dedman, J. T. Froeschke, E. A. Seubert, A. E. Jefferson, A. M. Kroetz, J. F.  
 516 Mareska, and S. P. Powers.  
 517 2020. Defining sex-specific suitability for a northern Gulf of Mexico shark assemblage.  
 518 *Front. Mar. Sci.* 7(35). doi: 10.3389/fmars.2020.00035.  
 519

520 Elith, J., J. R. Leathwick, and T. Hastie.  
 521 2008. A working guide to boosted regression trees. *J. Anim. Ecol.* 77:802–813. doi:  
 522 10.1111/j.1365-2656.2008.01390.x  
 523

524 Goethel, D. R., Quinn, T. J. and Cadrin, S. X.  
 525 2011. Incorporating spatial structure in stock assessment: movement modeling in marine  
 526 fish population dynamics. *Rev. Fish. Sci.* 19(2), pp.119-136.  
 527

528 Hanley, J. A., and B. J. McNeil.  
 529 1982. The meaning and use of the area under a Receiver Operating Characteristic (ROC)  
 530 curve. *Radiology* 143: 29-36.  
 531

532 Hardin, J. W., and J. Hilbe.  
 533 2007. *Generalized linear models and extensions*. Stata Press.  
 534

535 Hartig, F.  
 536 2017. DHARMA: residual diagnostics for hierarchical (multi-level/mixed) regression  
 537 models. R package version 0.1, 5.  
 538

539 Hijmans, R. J., and J. Elith.  
 540 2013. *Species Distribution Modeling with R*. R CRAN Project. Vienna: R Foundation for  
 541 Statistical Computing.

542  
543 Hoenig, J. M.  
544 1983. Empirical use of longevity data to estimate mortality rates. Fish. Bull. 82:898–903.  
545  
546 Jefferson, A. E., R. J. Allman, A. E. Pacicco, J. S. Franks, F. J. Hernandez, M. A. Albins, S. P.  
547 Powers, R. L. Shipp, and J. M. Drymon.  
548 2019. Age and growth of gray triggerfish (*Balistes capricus*) from a north-central Gulf of  
549 Mexico artificial reef zone. Bull. Mar. Sci. 95:177–195.  
550  
551 Katsanevakis, S., and C. D. Maravelias.  
552 2008. Modelling fish growth: multi-model inference as a better alternative to a priori using  
553 von Bertalanffy equation. Fish. Fish. 9:178–187.  
554  
555 Lane, J. Q., P. T. Raimondi, and R. M. Kudela.  
556 2009. Development of a logistic regression model for the prediction of toxigenic *Pseudo-*  
557 *nitzschia* blooms in Monterey Bay. Calif. Mar. Ecol. Prog. Ser. 383:37–51.  
558  
559 Livernois, M. C., Powers, S. P., Albins, M. A. and Mareska, J. F.  
560 2020. Habitat associations and co-occurrence patterns of two estuarine-dependent predatory  
561 fishes. Mar. Coast. Fish 12(1), pp.64-77.  
562  
563 Lo, N. C. H., L. D. Jacobson, and J. L. Squire.  
564 1992. Indices of relative abundance from fish spotter data based on delta-lognormal  
565 models. Can. J. Fish. Aquat. Sci. 49, 2515–2526. doi: 10.1139/f92-278.  
566  
567 Lowerre-Barbieri, S. K., Barbieri, L. R., Flanders, J. R., Woodward, A. G., Cotton, C. F. and  
568 Knowlton, M. K.,  
569 2008. Use of passive acoustics to determine red drum spawning in Georgia waters. Trans.  
570 Am. Fish. 137(2), pp.562-575.  
571  
572 Lowerre-Barbieri, S. K., Walters Burnsed, S. L. and Bickford, J. W.  
573 2016. Assessing reproductive behavior important to fisheries management: a case study with  
574 red drum, *Sciaenops ocellatus*. Ecol. Appl. 26(4), pp.979-995.  
575  
576 Lowerre-Barbieri, S. K., Tringali, M. D., Shea, C. P., Walters Burnsed, S., Bickford, J., Murphy,  
577 M. and Porch, C.  
578 2019. Assessing red drum spawning aggregations and abundance in the Eastern Gulf of  
579 Mexico: a multidisciplinary approach. ICES J. Mar. Sci. 76(2), pp.516-529.  
580  
581 Lüdecke, D., D. Makowski, and P. Waggoner.  
582 2019. performance: Assessment of regression models performance. CRAN.  
583  
584 Lynch, P.D., Methot, R. D. and Link, J. S.  
585 2018. Implementing a Next Generation Stock Assessment Enterprise: An Update to the  
586 NOAA Fisheries Stock Assessment Improvement Plan.  
587

588 MRIP (Marine Recreational Information Program).  
589 2021. Recreational fishing data and statistics queries. National Oceanic and Atmospheric  
590 Administration Fisheries, Silver Spring, Maryland.  
591  
592 Nelson, T. R., A. E. Jefferson, P. T. Cooper, C. A. Buckley, K. L. Heck, and J. Mattila.  
593 2018. Eurasian perch *Perca fluviatilis* growth and fish community structure, inside and  
594 outside a marine-protected area in the Baltic Sea. *Fish. Manag. Ecol.* 25:172–185.  
595  
596 Newman, D., Berkson, J. and Suatoni, L.  
597 2015. Current methods for setting catch limits for data-limited fish stocks in the United  
598 States. *Fish. Res.* 164, pp.86-93.  
599  
600 Ogle, D. H.  
601 2016. Introductory fisheries analyses with R. CRC Press, Boca Raton, FL.  
602  
603 Ogle, D. H., P. Wheeler, and A. Dinno.  
604 2020. FSA: Fisheries Stock Analysis. R package version 0.8.27. Available:  
605 <https://github.com/droglenc/FSA>.  
606  
607 Olney, J. E. and Hoenig, J. M.  
608 2001. Managing a fishery under moratorium: assessment opportunities for Virginia's stocks  
609 of American shad. *Fisheries*, 26(2), pp.6-12.  
610  
611 Parisien, M. A., and M. A. Moritz.  
612 2009. Environmental controls on the distribution of wildfire at multiple spatial scales. *Ecol.*  
613 *Monogr.* 79:127–154. doi: 10.1890/07-1289.1  
614  
615 Pauly, D.  
616 1980. On the interrelationships between natural mortality, growth parameters, and mean  
617 environmental temperature in 175 fish stocks. *ICES J. Mar. Sci.* 39:175–192.  
618  
619 Powers, S. P., C. L. Hightower, J. M. Drymon, and M. W. Johnson.  
620 2012. Age composition and distribution of Red Drum (*Sciaenops ocellatus*) in offshore  
621 waters of the north central Gulf of Mexico: an evaluation of a stock under a federal  
622 harvest moratorium. *Fish. Bull.* 110(3):283–292.  
623  
624 Quantum GIS Development Team  
625 2019. Quantum GIS Geographic Information System, v3.8.1.  
626  
627 R Core Team.  
628 2020. R: A language and environment for statistical computing. R Foundation for Statistical  
629 Computing, Vienna, Austria.  
630  
631 Reyier, E. A., Lowers, R. H., Scheidt, D. M. and Adams, D. H.

632 2011. Movement patterns of adult red drum, *Sciaenops ocellatus*, in shallow Florida lagoons  
633 as inferred through autonomous acoustic telemetry. *Environ. Biol. Fishes.* 90(4),  
634 pp.343-360.

635  
636 Rooker, J. R., G. W. Stunz, S. A. Holt, and T. J. Minello.  
637 2010. Population connectivity of red drum in the northern Gulf of Mexico. *Mar. Ecol. Prog.*  
638 *Ser.* 407:187-196.

639  
640 Sagarese, S. R., Harford, W. J., Walter, J. F., Bryan, M. D., Isely, J. J., Smith, M. W., Goethel,  
641 D. R., Rios, A. B., Cass-Calay, S. L., Porch, C. E. and Carruthers, T. R.  
642 2019. Lessons learned from data-limited evaluations of data-rich reef fish species in the Gulf  
643 of Mexico: implications for providing fisheries management advice for data-poor  
644 stocks. *Can. J. Fish. Aquat. Sci.* 76(9), pp.1624-1639.

645  
646 SEDAR.  
647 2016. SEDAR49: Gulf of Mexico Data-limited Species Stock Assessment Report [online].  
648 SEDAR, North Charleston, South Carolina. Available from [sedarweb.org](http://sedarweb.org) [accessed  
649 September 2021].

650  
651 Smith, M. W., A. Y. Then, C. Wor, G. Ralph, K. H. Pollock, and J. M. Hoenig.  
652 2012. Recommendations for catch-curve analysis. *N. Am. J. Fish. Manag.* 32(5):956–967.

653  
654 Then, A. Y., J. M. Hoenig, N. G. Hall, and D. A. Hewitt.  
655 2015. Evaluating the predictive performance of empirical estimators of natural mortality rate  
656 using information on over 200 fish species. *ICES J. Mar. Sci.* 72:82–92.

657  
658 Tuckey, T., N. Yochum, J. Hoenig, J. Lucy, and J. Cimino.  
659 2007. Evaluating localized vs. large-scale management: the example of tautog in Virginia.  
660 *Fisheries* 32(1):21–28.

661  
662 VanderKooy, S., J. S. Elzey, J. Gilmore, and J. Kipp, editors.  
663 2020. A practical handbook for determining the age of Gulf of Mexico and Atlantic Coast  
664 fishes, 3<sup>rd</sup> edition. Gulf States Marine Fisheries Commission, Ocean Springs, MS.

665  
666 von Bertalanffy, L.  
667 1938. A quantitative theory of organic growth (inquiries on growth laws II). *Hum. Biol.*  
668 10:181–213.

669  
670 Winner, B. L., Flaherty-Walia, K. E., Switzer, T. S. and Vecchio, J. L.  
671 2014. Multidecadal evidence of recovery of nearshore red drum stocks off west-central  
672 Florida and connectivity with inshore nurseries. *N. Am. J. Fish. Manag.* 34(4),  
673 pp.780-794.

674 **Tables**

675 **Table 1** – von Bertalanffy growth parameters for combined (sexes pooled, including unknown  
 676 sex) and sex-specific red drum age data.  $L_{\infty}$  = mean asymptotic length in millimeters,  $K$  = Brody  
 677 growth rate coefficient in years<sup>-1</sup>,  $t_0$  = hypothetical age at which length equals 0 in years, and SE  
 678 = standard error.

	$L_{\infty} \pm SE$	$K \pm SE$	$t_0 \pm SE$
<b>Combined</b>	950.45 ± 2.35	0.31 ± 0.01	-0.26 ± 0.03
<b>Female</b>	969.63 ± 3.42	0.30 ± 0.01	-0.35 ± 0.05
<b>Male</b>	932.71 ± 3.78	0.30 ± 0.01	-0.45 ± 0.06

679

680

Draft in Review

681 **Table 2** – Seasonal percent contribution of the three most influential factors identified by the boosted regression trees. The AUC score  
 682 assesses model ability to discriminate species presence and absence (Hanley and McNeil 1982), with a value of 0.9 considered a ‘very  
 683 good score’ (Lane et al. 2009).

Season	Training data AUC	CV AUC score $\pm$ SE	Marginal Effect 1		Marginal Effect 2		Marginal Effect 3	
			Variable	%	Variable	%	Variable	%
Spring	0.90	0.86 $\pm$ 0.01	Surface northward velocity	26.2	Surface temperature	20.7	Depth	14.7
Summer	0.90	0.85 $\pm$ 0.01	Surface northward velocity	25.8	Surface temperature	20.4	Depth	14.6
Autumn	0.90	0.86 $\pm$ 0.01	Surface northward velocity	25.8	Surface temperature	20.4	Depth	14.4

684

685 **Figures**

686 **Figure 1** – Bottom longline (black shaded) and gillnet (blue shaded) study regions. The red  
687 dashed line indicates the boundary between state and federal waters.

688 **Figure 2** – Catch per unit effort (CPUE, red drum, hooks<sup>-1</sup> hour<sup>-1</sup>) for red drum from the bottom  
689 longline survey during spring, summer, and autumn of 2006 – 2018. Shaded circles increase with  
690 CPUE, and X indicates effort with no red drum catch.

691 **Figure 3** – A) Length frequency distributions for red drum (sexes combined) encountered on the  
692 bottom longline. B) Length frequency distributions for female and male red drum examined for  
693 age and growth analyses from bottom longline and gillnet data sets. The dashed line represents  
694 size at 50% maturity according to Bennetts et al. (2019).

695 **Figure 4** – Combined (A) and sex-specific (B) von Bertalanffy growth curves for red drum  
696 sampled during the present study.

697 **Figure 5** – Nominal (individuals 100 hooks<sup>-1</sup> hour<sup>-1</sup>, open circles) and standardized (filled  
698 circles) CPUE of red drum from the bottom longline survey, 2006 – 2018. Approximately 100  
699 stations per year (mean = 100, SD = 22, range 80 – 143) were sampled. Median values are shown  
700 in the standardized index. For 2009, there is no standardized CPUE estimate due to a lack of  
701 positive catch data with corresponding abiotic measurements from that year.

702 **Figure 6** – Marginal effect plots for the variables identified by the BRTs as the most influential  
703 in predicting red drum relative abundance in spring (A–C), summer (D–F), and autumn (G–I).

704 **Figure 7** – Predicted relative abundance from BRT models for red drum in spring (A), summer  
705 (B), and autumn (C). Light shades indicate areas of low predicted abundance and dark shades  
706 indicate areas of high predicted abundance.

707 **Figure 8** –Red drum harvest data for Mississippi/Alabama (A) and Florida (B), 2006-2018. The  
708 dashed line represents size at 50% maturity according to Bennetts et al. (2019). Data are from the  
709 NOAA Marine Recreational Information Program web site (MRIP 2021).

710 **Supplemental Figure 1** – Residual diagnostic plots for examining model fit were created using  
711 the DHARMA package (Hartig 2017), which calculates quantile regression to compare the  
712 empirical 0.25, 0.50 and 0.75 quantiles with the theoretical 0.25, 0.50 and 0.75 quantiles. Any  
713 significant deviation from the expected quantile would be indicated in red.

714 **Supplemental Figure 2** – Coefficient of variation of predicted relative abundance from BRT  
715 models for red drum in spring (A), summer (B), and autumn (C). Light shades indicate areas of  
716 low predicted abundance and dark shades indicate areas of high predicted abundance.

Fig1

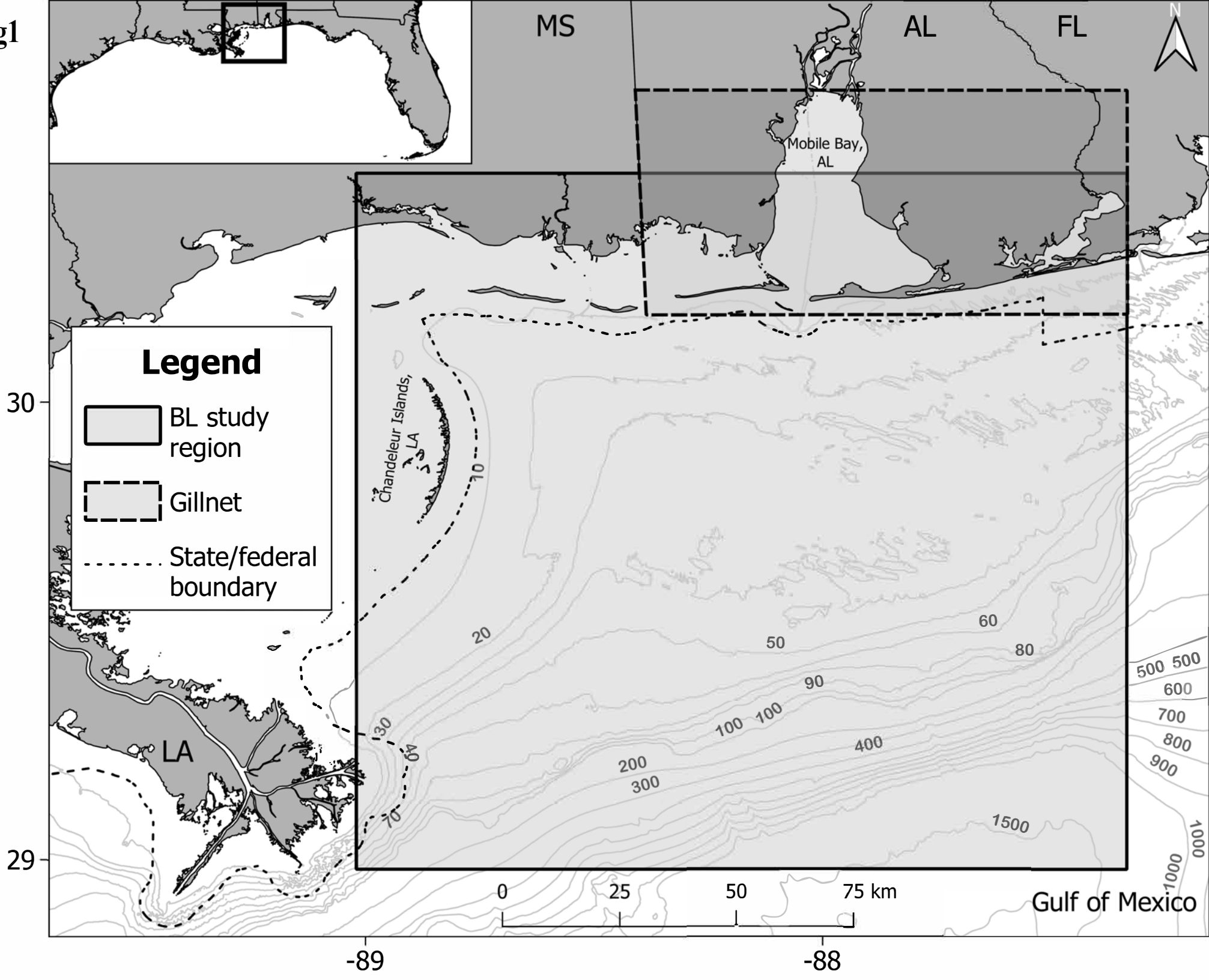
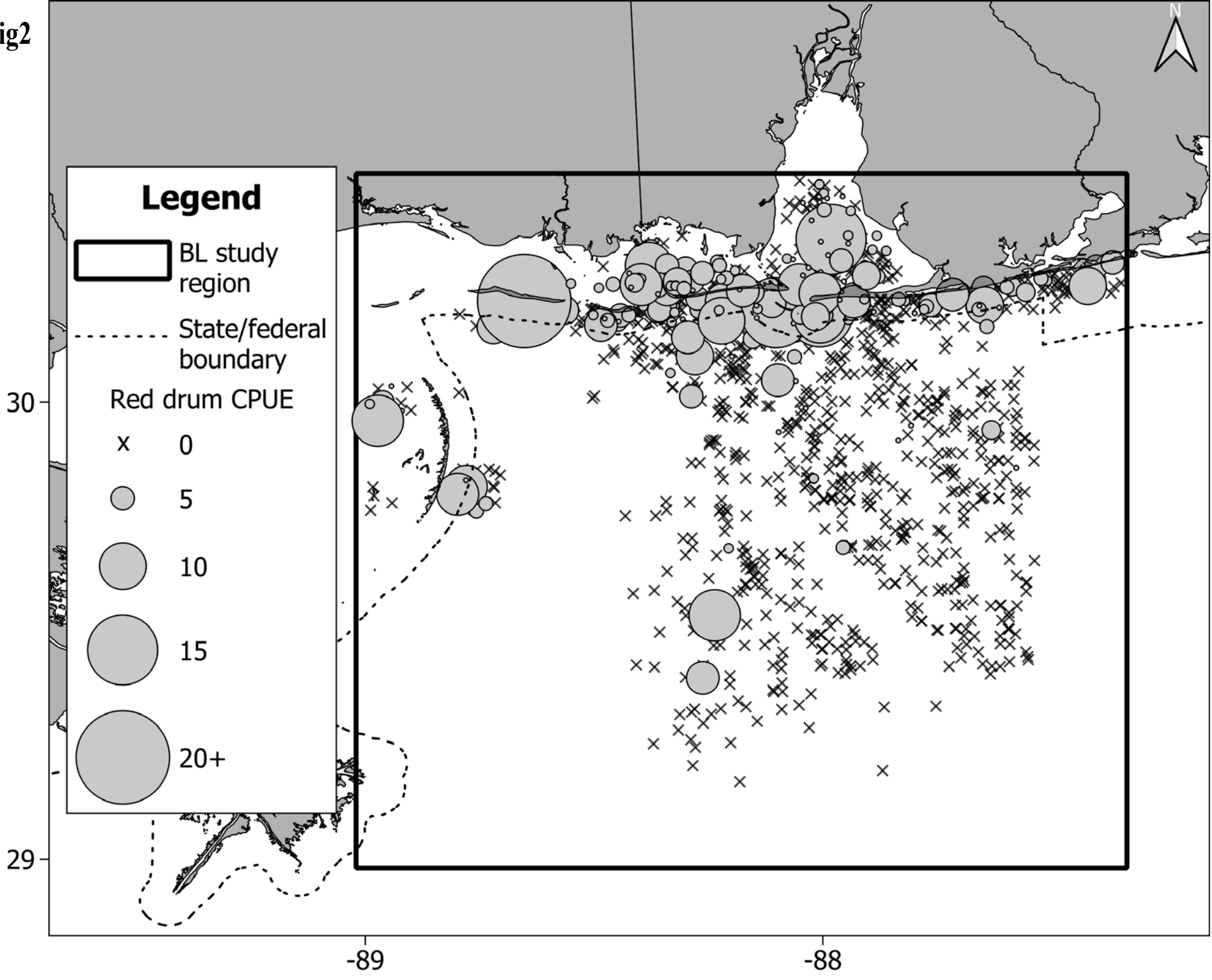


Fig2



**Fig3**

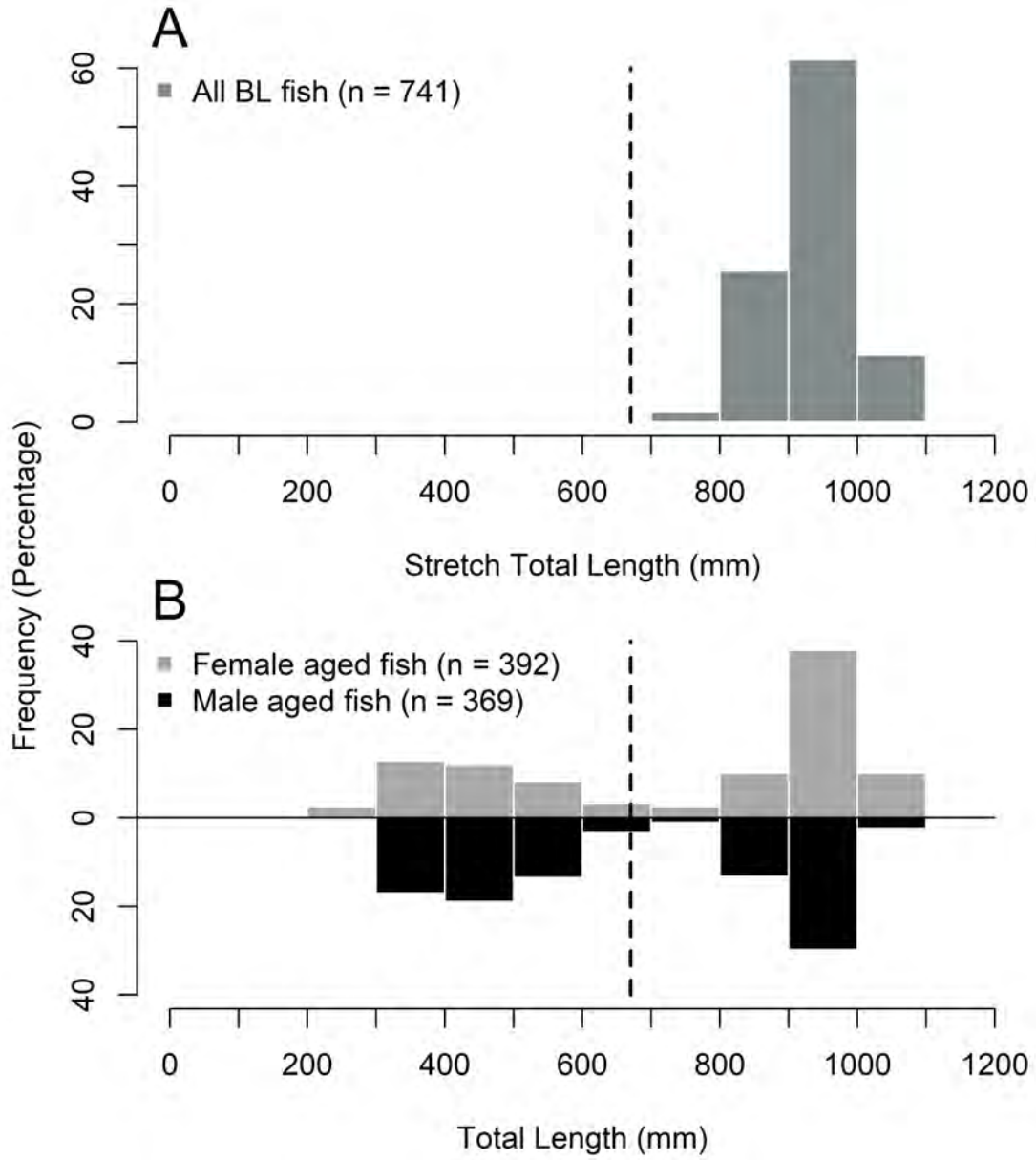


Fig4

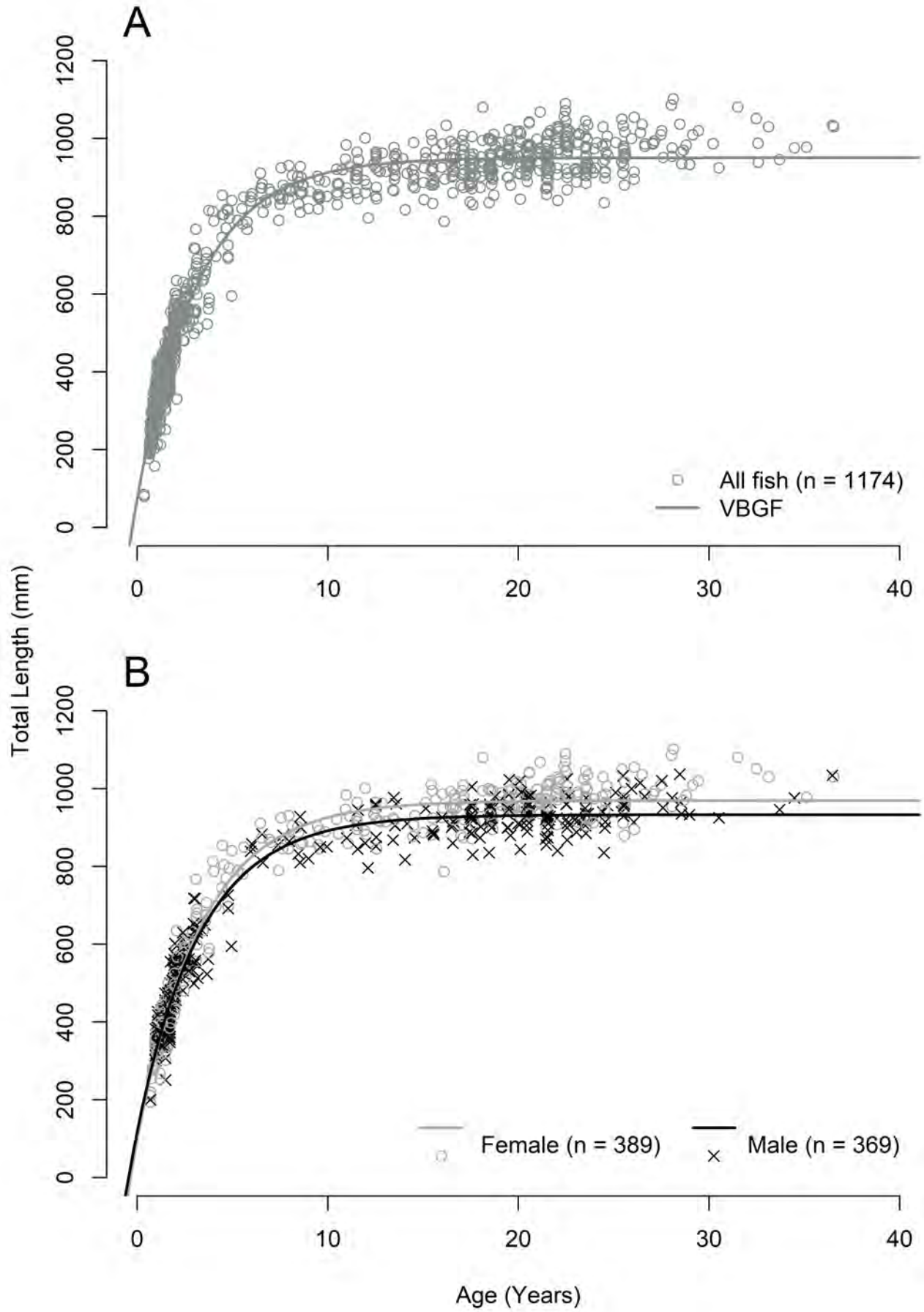
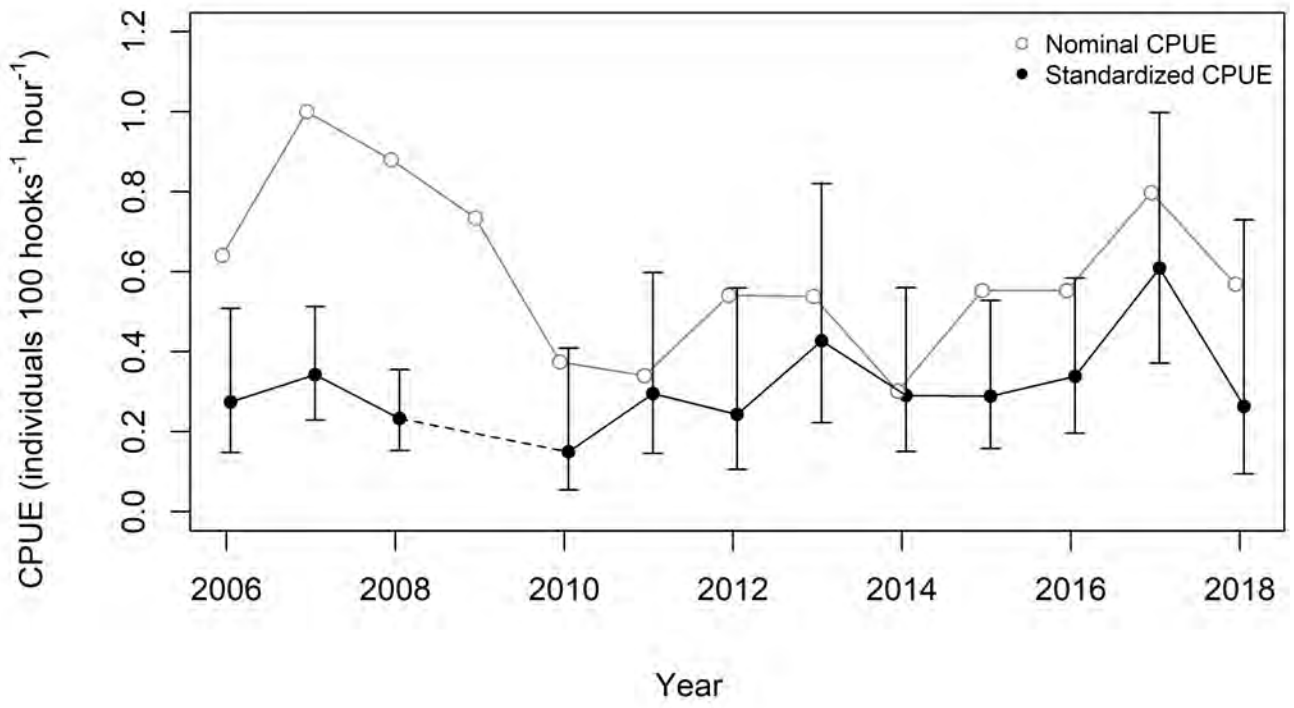


Fig5



**Fig6**

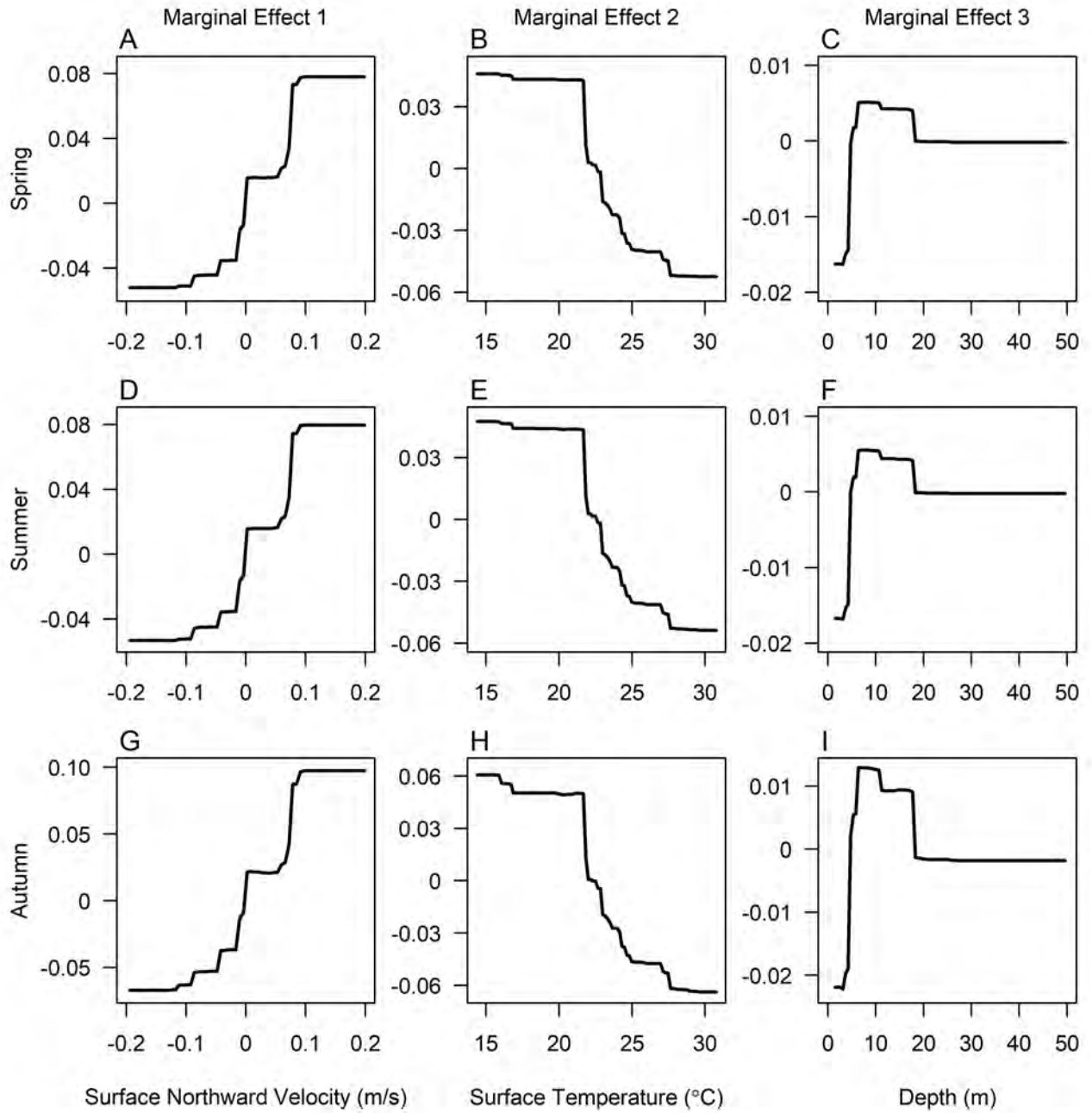


Fig7

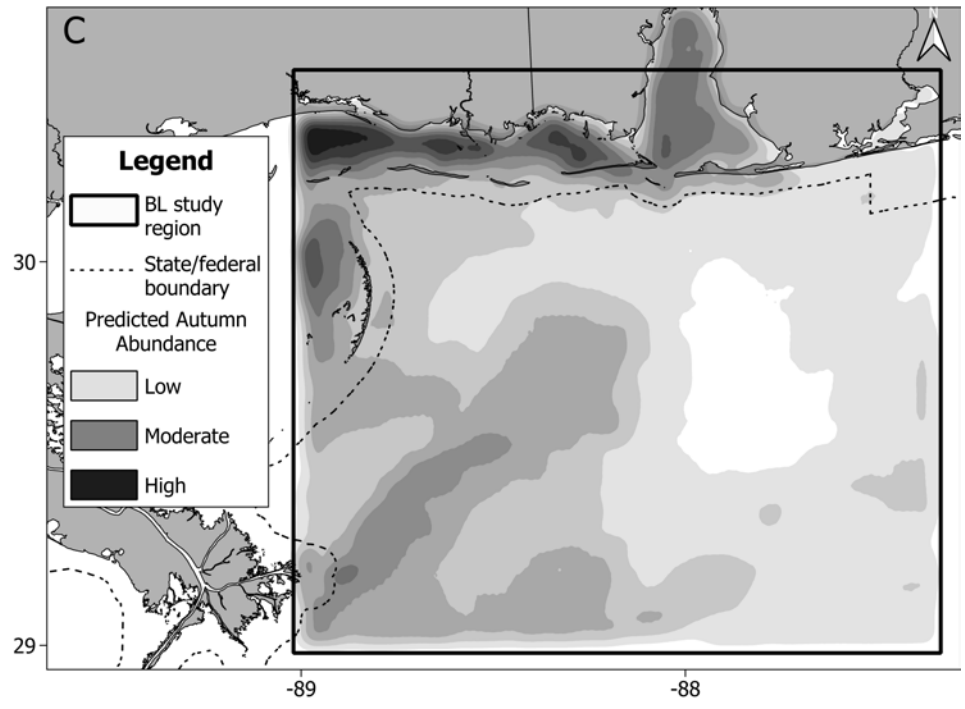
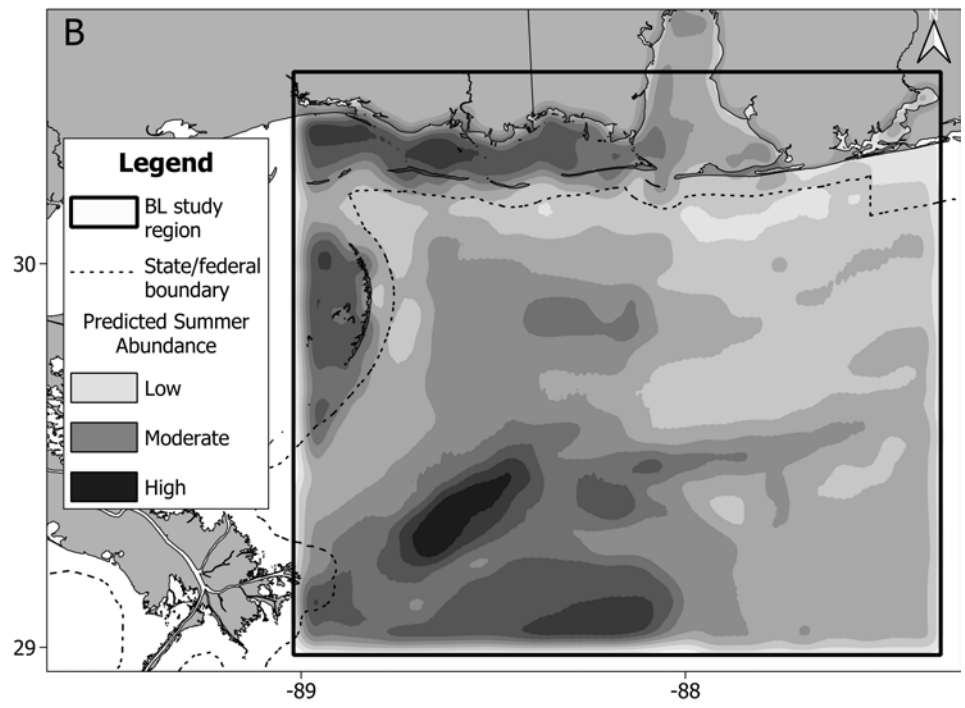
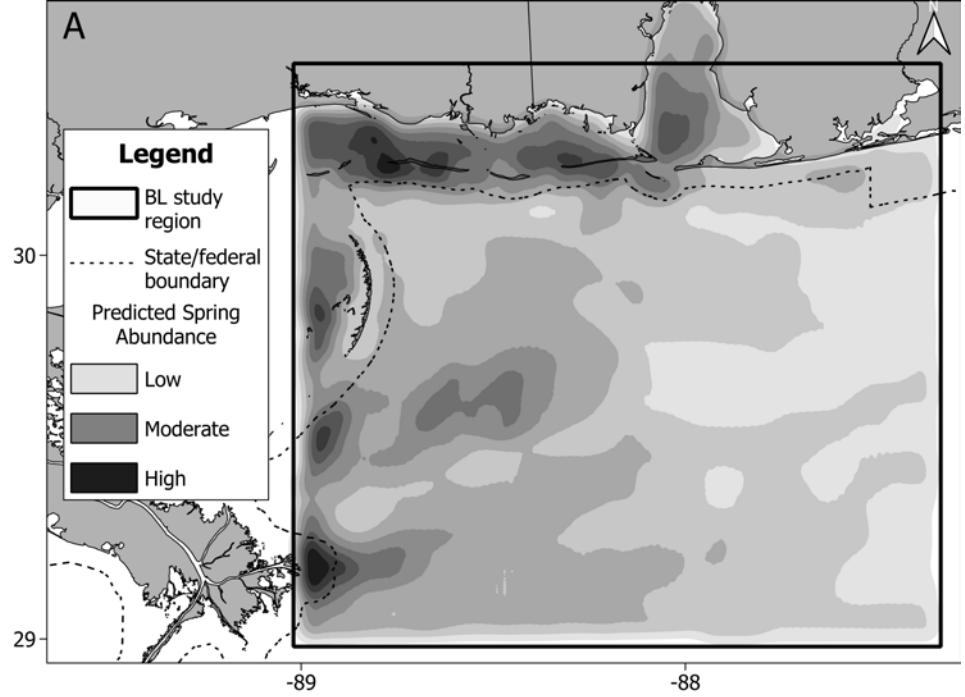
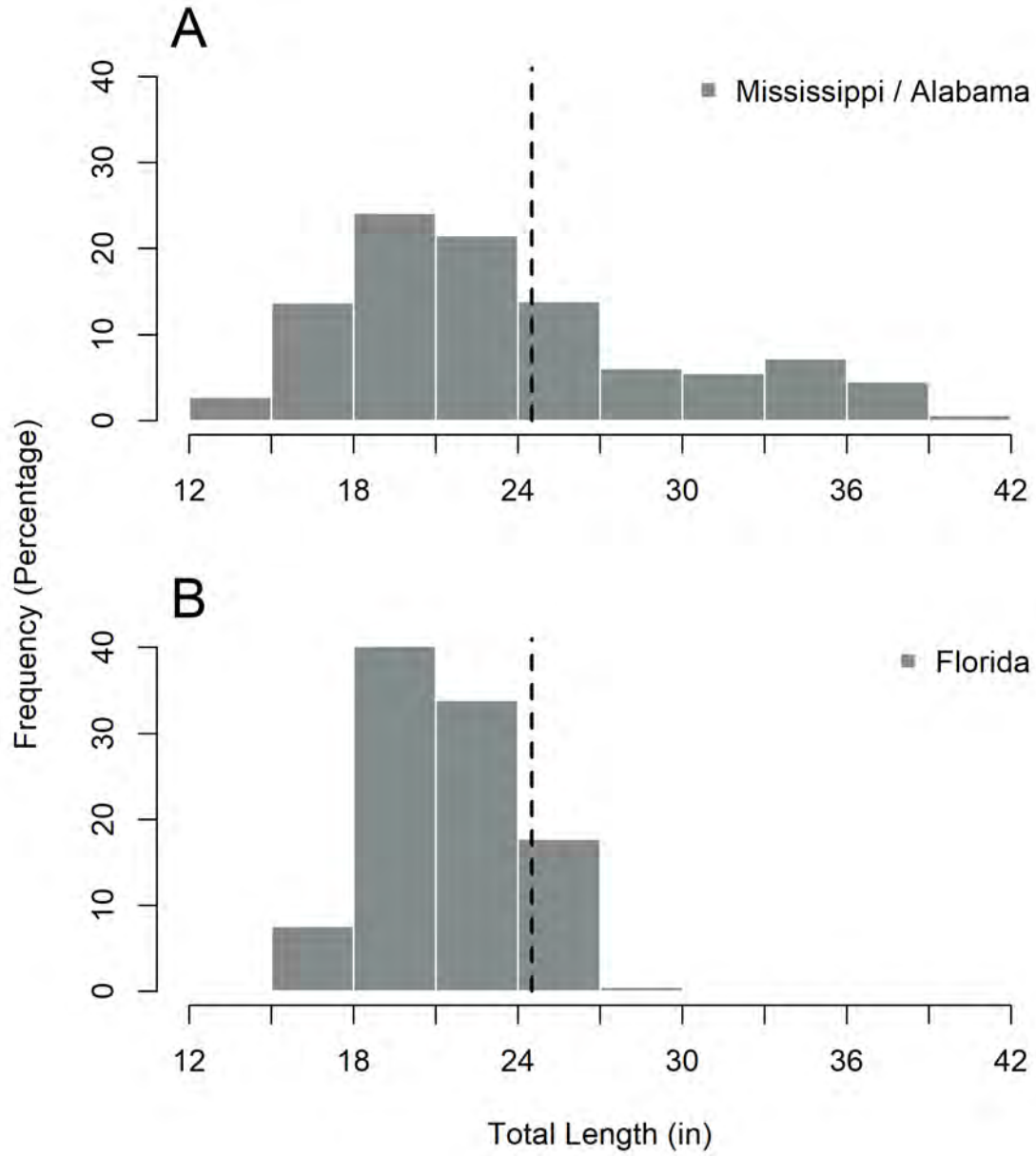


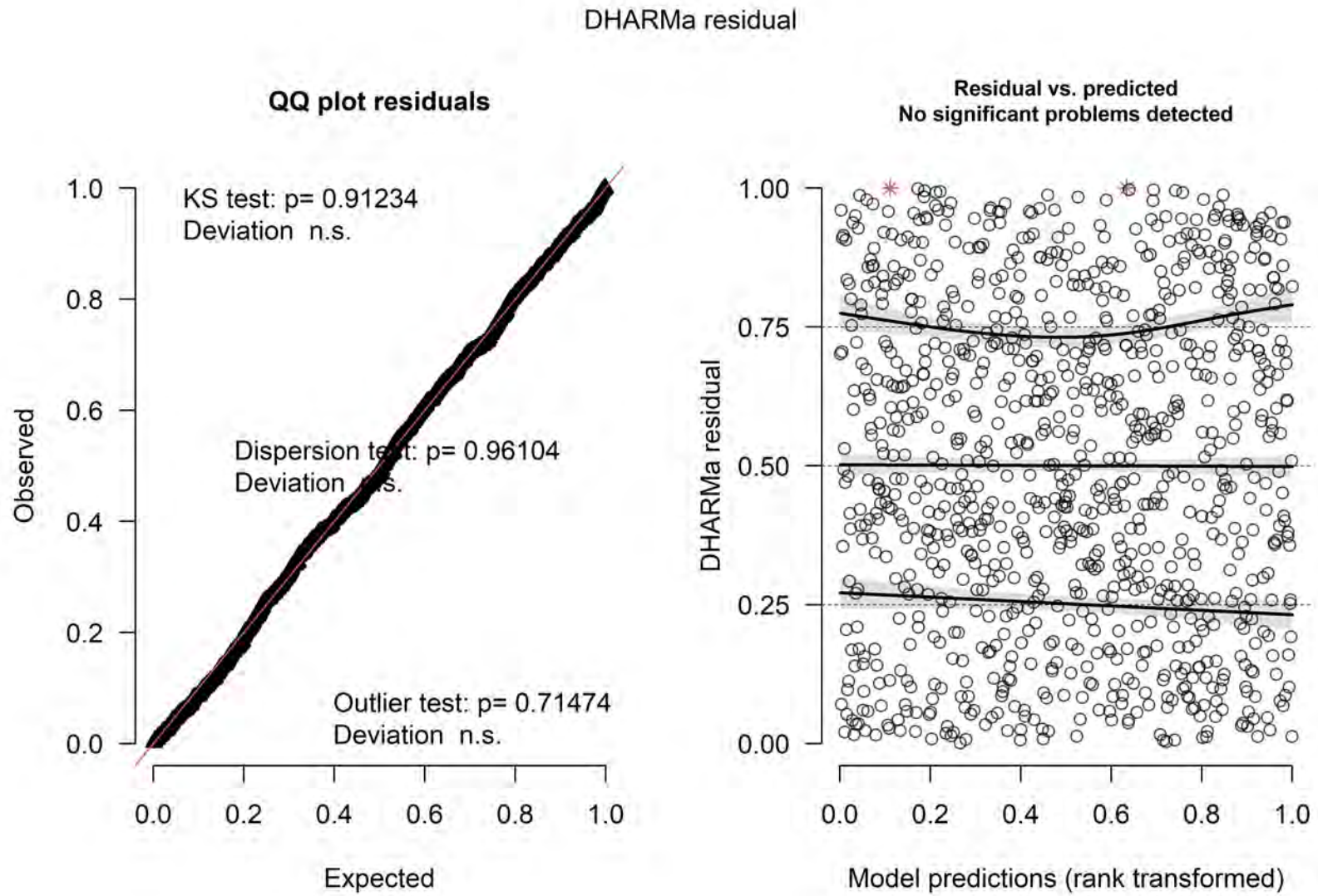
Fig8



**Supplemental Table 1:** Mean values and range for potential predictor variables included in the boosted regression trees (Table from Drymon et al. 2020)

<b>Predictor</b>	<b>Source</b>	<b>Mean <math>\pm</math> SE</b>	<b>Range</b>
Surface temperature ( $^{\circ}$ C)	HYCOM	25.788 $\pm$ 0.110	15.090 to 33.500
Bottom temperature ( $^{\circ}$ C)	HYCOM	24.202 $\pm$ 0.109	14.280 to 31.970
Surface salinity (psu)	HYCOM	30.666 $\pm$ 0.139	0.004 to 36.013
Bottom salinity (psu)	HYCOM	31.935 $\pm$ 0.152	0.004 to 38.349
Surface eastward velocity, u (m/s)	HYCOM	0.027 $\pm$ 0.004	-0.465 to 0.538
Bottom eastward velocity, u (m/s)	HYCOM	0.020 $\pm$ 0.002	-0.239 to 0.219
Surface northward velocity, v (m/s)	HYCOM	-0.001 $\pm$ 0.003	-0.505 to 0.432
Bottom northward velocity, v (m/s)	HYCOM	0.003 $\pm$ 0.001	-0.353 to 0.232
Surface upward velocity, w (m/s)	HYCOM	-2.513e <sup>-8</sup> $\pm$ 9.374e <sup>-8</sup>	-1.710e <sup>-5</sup> to 1.790e <sup>-5</sup>
Bottom upward velocity, w (m/s)	HYCOM	1.410e <sup>-6</sup> $\pm$ 8.354e <sup>-7</sup>	-4.005e <sup>-4</sup> to 3.023e <sup>-4</sup>
Sea surface height (m)	HYCOM	-0.005 $\pm$ 0.003	-0.312 to 0.329
Bottom DO (mg/l)	NOAA	5.604 $\pm$ 0.048	0.224 to 12.161
Depth (m)	USGS	22.518 $\pm$ 0.813	1.500 to 635.00
Substrate grain size (mm)	USGS	0.097 $\pm$ 0.006	0.001 to 7.172
Daylength (min)	Calculated	772.557 $\pm$ 1.637	622.083 to 846.800
Distance from shore (km)	Calculated	20.798 $\pm$ 0.712	0.002 to 101.715

SFig1



SFig2

